

IMMUNOBIOLOGY AND IMMUNOTHERAPY

Targeting intracellular WT1 in AML with a novel RMF-peptide-MHC-specific T-cell bispecific antibody

Christian Augsberger,^{1,2,*} Gerulf Hänel,^{1,2,*} Wei Xu,³ Vesna Pulko,³ Lydia Jasmin Hanisch,³ Angeliqe Augustin,⁴ John Challier,³ Katharina Hunt,⁵ Binje Vick,⁵ Pier Eduardo Rovatti,⁶ Christina Krupka,^{1,2} Maurine Rothe,^{1,2} Anne Schönle,³ Johannes Sam,³ Emmanuelle Lezan,⁴ Axel Ducret,⁴ Daniela Ortiz-Franyuti,⁴ Antje-Christine Walz,⁴ Jörg Benz,⁴ Alexander Bujotzek,⁷ Felix S. Lichtenegger,⁷ Christian Gassner,⁷ Alejandro Carpy,⁷ Victor Lyamichev,⁸ Jigar Patel,⁸ Nikola Konstandin,¹ Antje Tunger,^{9,10} Marc Schmitz,^{9,10,11} Michael von Bergwelt-Baildon,^{1,11} Karsten Spiekermann,^{1,11} Luca Vago,^{6,12} Irmela Jeremias,^{5,13,14} Estelle Marrer-Berger,⁴ Pablo Umaña,³ Christian Klein,³ and Marion Subklewe^{1,2,11}

¹Department of Medicine III, University Hospital, LMU Munich, Munich, Germany; ²Laboratory for Translational Cancer Immunology, Gene Center, LMU Munich, Munich, Germany; ³Roche Pharma Research & Early Development, Roche Innovation Center Zurich, Schlieren, Switzerland; ⁴Roche Pharma Research & Early Development, Roche Innovation Center Basel, Basel, Switzerland; ⁵Research Unit Apoptosis in Hematopoietic Stem Cells (AHS), Helmholtz Center Munich, German Research Center for Environmental Health, Munich, Germany; ⁶Unit of Immunogenetics, Leukemia Genomics and Immunobiology, IRCCS San Raffaele Scientific Institute, Milan, Italy; ⁷Roche Pharma Research & Early Development, Roche Innovation Center Munich, Penzberg, Germany; ⁸Nimble Therapeutics, Madison, WI; ⁹Institute of Immunology, Faculty of Medicine Carl Gustav Carus, TU Dresden, Dresden, Germany; ¹⁰National Center for Tumor Diseases, Partner Site Dresden, Dresden, Germany; ¹¹German Cancer Consortium (DKTK) and German Cancer Research Center (DKFZ), Heidelberg, Germany; ¹²Hematology and Bone Marrow Transplantation Unit, IRCCS San Raffaele Scientific Institute, Milan, Italy; ¹³German Cancer Consortium (DKTK), Partner Site Munich, Munich, Germany; and ¹⁴Department of Pediatrics, Dr von Hauner Children's Hospital, Ludwig Maximilian University (LMU), Munich, Germany

KEY POINTS

- A T-cell bispecific antibody targeting intracellular WT1 presented on HLA-A2 for treatment of AML is characterized in vitro and in vivo.
- The novel, clinical-stage WT1-TCB mediated high-level killing of primary AML cells, which was enhanced by the addition of lenalidomide.

Antibody-based immunotherapy is a promising strategy for targeting chemoresistant leukemic cells. However, classical antibody-based approaches are restricted to targeting lineage-specific cell surface antigens. By targeting intracellular antigens, a large number of other leukemia-associated targets would become accessible. In this study, we evaluated a novel T-cell bispecific (TCB) antibody, generated by using CrossMAb and knob-into-holes technology, containing a bivalent T-cell receptor-like binding domain that recognizes the RMFPNAPYL peptide derived from the intracellular tumor antigen Wilms tumor protein (WT1) in the context of HLA-A*02. Binding to CD3ε recruits T cells irrespective of their T-cell receptor specificity. WT1-TCB elicited antibody-mediated T-cell cytotoxicity against AML cell lines in a WT1- and HLA-restricted manner. Specific lysis of primary acute myeloid leukemia (AML) cells was mediated in ex vivo long-term cocultures by using allogeneic (mean ± standard error of the mean [SEM] specific lysis, 67 ± 6% after 13-14 days; n = 18) or autologous, patient-derived T cells (mean ± SEM specific lysis, 54 ± 12% after 11-14 days; n = 8). WT1-TCB-treated T cells exhibited higher cytotoxicity against primary AML cells than

an HLA-A*02 RMF-specific T-cell clone. Combining WT1-TCB with the immunomodulatory drug lenalidomide further enhanced antibody-mediated T-cell cytotoxicity against primary AML cells (mean ± SEM specific lysis on days 3-4, 45.4 ± 9.0% vs 70.8 ± 8.3%; P = .015; n = 9-10). In vivo, WT1-TCB-treated humanized mice bearing SKM-1 tumors exhibited a significant and dose-dependent reduction in tumor growth. In summary, we show that WT1-TCB facilitates potent in vitro, ex vivo, and in vivo killing of AML cell lines and primary AML cells; these results led to the initiation of a phase 1 trial in patients with relapsed/refractory AML (#NCT04580121).

Introduction

Recruitment of T cells to tumor cells by T-cell-recruiting antibody constructs is a proven and effective way to treat cancer independently of preexisting tumor-specific T cells.¹⁻⁵ Blinatumomab, a bispecific T-cell engager (BiTE, Amgen, Thousand Oaks, CA) consisting of 2 single-chain variable fragments directed against CD3×CD19, has been approved for the treatment of Philadelphia chromosome-positive and -negative, relapsed or refractory B-cell

precursor acute lymphoblastic leukemia.^{6,7} Several other bispecific antibodies having different targets, mainly lineage antigens, are currently being evaluated in clinical trials.⁸⁻¹⁵ However, these targets are indiscriminate between healthy and tumor cells. Whereas a depleted healthy compartment is manageable in cases of B-cell malignancy, targeting lineage antigens in myeloid malignancies is associated with the risk of hematotoxicity and poses a potential safety concern.^{16,17}

In contrast, the intracellular antigen Wilms tumor protein (WT1) displays a rather restricted expression profile. It is a transcriptional and post-transcriptional regulator playing crucial roles in embryonic development and organ homeostasis.^{18,19} In adults, WT1 expression is restricted to a few tissues (kidney podocytes; Sertoli and granulosa cells in the testes and ovaries, respectively; a few mesothelial cells; and 1% of bone marrow cells).¹⁸⁻²¹ In addition to its physiological role in healthy cells, WT1 has reportedly contributed to the development of cancer, although its specific function in relation to this observation is not completely understood. WT1 is overexpressed in leukemias and solid cancers and is therefore widely regarded as a potential target antigen for immunotherapeutic approaches.^{22,23}

Targeting intracellular antigens with antibody constructs requires their binding to an HLA-restricted peptide epitope. For WT1, several epitopes have been identified. In particular, the non-peptide WT1₁₂₆₋₁₃₄ (RMFPNAPYL; "RMF"), which is presented on HLA-A*02, has been targeted in the context of several cancer entities, including acute myeloid leukemia (AML).²⁴⁻²⁶

Few approaches for targeting WT1 have reached clinical development. In a phase 1/2 clinical trial, adoptive transfer of donor-derived ex vivo-expanded, WT1-specific CD8⁺ T cells was shown to be safe and to result in antileukemic activity.²⁷ Adoptively transferred WT1_{RMF}-specific T-cell receptor (TCR)-transgenic T cells were also shown to be safe and to persist in patients with refractory AML or high-risk myelodysplastic syndrome taking part in a phase 1 clinical trial; they were able to prevent relapse if administered posttransplant, supporting further evaluation of this target.^{28,29} In a phase 2 clinical trial for postremission therapy of AML, vaccination with dendritic cells electroporated with WT1 messenger RNA (mRNA) was shown to reduce the risk of relapse after standard chemotherapy.^{30,31} Various WT1 peptide vaccines have been tested in phase 1 and phase 2 clinical trials.³² In preclinical studies, the therapeutic efficacy of WT1-specific chimeric antigen receptor T cells was shown in a xenograft mouse model.³³ Antibody-based immunotherapeutic approaches with TCR-mimicking T cell-recruiting antibodies have also been developed but could not be translated from mouse models into the clinic.³⁴⁻³⁷ WT1 has thus been validated as a safe and promising target antigen independently of the genetic subtype of AML.

In the current study, we evaluated a novel T-cell bispecific (TCB) antibody based on the TCR-like antibody 11D06 for the immunotherapy of AML. The TCB is directed against WT1 by recognition of the WT1_{RMF} peptide, which is processed and presented on HLA-A*02. In contrast to the aforementioned approaches, the construct relies on bivalent recognition of the tumor antigen, which is facilitated by an additional Fab domain fused to the N terminus of the VL domain of a CrossMab^{VH-VL}.³⁸⁻⁴⁰ This results in a trivalent "2 + 1" immunoglobulin G (IgG) antibody for bivalent recognition of WT1-peptide major histocompatibility complexes (pMHC). Complementary monovalent binding to CD3 ϵ in the TCR complex recruits T cells irrespective of their specificity. The TCB is based on human IgG1 and contains a mutated Fc region with a P329G LALA mutation; this confers extended half-life properties but excludes complement-dependent cellular cytotoxicity and antibody-dependent cellular cytotoxicity. Upon crosslinking, T cells are activated to form an immunologic synapse, which induces

apoptosis in tumor cells via the perforin/granzyme apoptosis pathway.⁴¹

Methods

Patients

Peripheral blood (PB) or bone marrow samples were collected from healthy donors (HDs) and patients with AML at primary diagnosis, relapse, or complete remission after written informed consent was received in accordance with the Declaration of Helsinki and approval was granted by the Institutional Review Board of the Ludwig-Maximilian-Universität (Munich, Germany).

WT1-TCB antibody generation and selection

Antibodies specific for the WT1-RMF peptide HLA-A*02 complex were generated by using phage display using standard protocols (further details are given in the supplemental Data, available on the *Blood* Web site).⁴² Of 34 complex-recognizing clones, the 11D06 antibody was selected due to its selectivity profile and characterization in cell assay, and reformatted into a trivalent 2 + 1 IgG TCB antibody for bivalent recognition of the WT1-pMHC complex and monovalency for the CD3 ϵ chain of the TCR. This was facilitated by fusion of a second Fab domain to the N terminus of the VL domain of the anti-CD3 ϵ Fab, resulting in a heterotrimeric CrossMab^{VH-VL}.³⁸ Introduction of a P329G LALA mutation⁴³ renders it inactive for complement-dependent cytotoxicity. For the work presented here, two different CD3 ϵ binders were incorporated, one based on the humanized antibody V9 derived from UCHT1, resulting in "WT1-TCB," and one related to the antibody Sp34 termed CH2527, yielding "WT1-TCB*." Both variants exhibited comparable potency in vitro and in vivo (supplemental Figure 1; Table 1). Accordingly, "WT1-TCB" is used throughout the article to refer to both constructs.

All antibodies were purified from transiently transfected HEK293-EBNA or CHO cells via protein A affinity chromatography and size exclusion chromatography.^{41,44,45} Affinities and avidities were characterized in surface plasmon resonance experiments by using a Biacore T200 (GE Healthcare, Chicago, IL).

Flow cytometry, cytokine quantification, and real-time polymerase chain reaction

Surface expression of CD33 (REA775), CD2 (REA972; both Miltenyi Biotec, Bergisch Gladbach, Germany), CD69 (FN50), PD1 (29F.1A12), TIM-3 (F38-2E2), CD45RA (HI100), and CCR7 (G43H7; all BioLegend, San Diego, CA) was assessed by using flow cytometry (CytoFLEX S, Beckman Coulter, Krefeld, Germany). Cytokine concentrations in cell culture supernatants were quantified by using the Human Th1/Th2 Cytokine Kit (BD Biosciences, Heidelberg, Germany). Alternatively, cytokines were measured on a Luminex 100 Analyzer (Bio-Rad, Hercules, CA) by using a custom ProcartaPlex panel (Invitrogen, Vienna, Austria). WT1 expression levels were quantified by using real-time quantitative polymerase chain reaction (qPCR), as previously described.⁴⁶

In vitro dose-response assays

T cells were isolated from PB of HDs and cocultured with tumor cell lines at an effector-to-target (E:T) ratio of 4:1 in the presence of various concentrations of WT1-TCB*. Mean specific lysis was assessed by flow cytometry and calculated relative to a control

Table 1. Affinities of WT1-TCB

pMHC affinity	pMHC avidity	CD3 affinity
$K_D = 50 \text{ nM (25}^\circ\text{C)}$ $k_a = 7.7 \pm 0.0 \times 10^5 \text{ 1/M s (37}^\circ\text{C)}$ $k_d = 3.7 \pm 0.0 \times 10^{-2} \text{ 1/s (37}^\circ\text{C)}$	0.45 nM	WT1-TCB $K_D = 3.7 \pm 0.8 \text{ nM (25}^\circ\text{C)}$ $11.3 \pm 0.1 \text{ nM (37}^\circ\text{C)}$ $k_a = 1.4 \pm 0.0 \times 10^5 \text{ 1/M s (37}^\circ\text{C)}$ $k_d = 1.6 \pm 0.0 \times 10^{-3} \text{ 1/s (37}^\circ\text{C)}$
		WT1-TCB* $K_D = 3.0 \pm 0.1 \text{ nM (25}^\circ\text{C)}$ $6.3 \pm 0.2 \text{ nM (37}^\circ\text{C)}$ $k_a = 2.1 \pm 0.1 \times 10^6 \text{ 1/M s (37}^\circ\text{C)}$ $k_d = 1.3 \pm 0.0 \times 10^{-2} \text{ 1/s (37}^\circ\text{C)}$

K_D , equilibrium dissociation constant; k_a , association rate constant; k_d , dissociation rate constant.

antibody construct (Ctrl-TCB) that recognizes a nontumor target derived from the human antibody germline repertoire.

Ex vivo short- and long-term cytotoxicity assays

Primary AML cells were thawed and pre-cultivated on a feeder layer of irradiated murine MS5 stromal cells in a 6-well plate for 3 to 4 days. For short-term cytotoxicity assays, cells were subsequently labeled with CellTrace Far Red (Life Technologies, Eugene, OR) to assess specific lysis. Cells were cocultured for 72 hours with autologous or HD peripheral blood mononuclear cells (PBMCs) at an E:T ratio of 5:1 and with various concentrations of WT1-TCB.

Ex vivo long-term cytotoxicity assays were performed as previously described.⁴⁷ After pre-cultivation on MS5 cells, primary AML cells were transferred onto a fresh feeder layer in a 96-well plate. WT1-TCB* was added at a concentration of 10 nM and HD T cells at an E:T ratio of 1:4 to 1:5 for 14 days.

Downstream TCR signaling

Downstream TCR signaling was measured by cocultivation of primary AML cells with NFAT Luciferase Reporter Jurkat cells (MilliporeSigma, Burlington, MA). Primary AML cells were precultured in the aforementioned culture system, followed by cocultivation with reporter cells in the presence of WT1-TCB* at an E:T ratio of 1:1 for 16 hours. Luminescence was induced by using the Bright-Glo Luciferase Assay System (Promega, Fitchburg, WI) and measured on an Infinite M1000 Plate Reader (Tecan, Männedorf, Switzerland).

In vivo studies with humanized mice

NSG mice (NOD.Cg-Prkdcscid-Il2rgtm1Wjl/SzJ) were humanized with human HLA-A*02⁺ CD34⁺ cord blood cells (details are provided in the supplemental Data). After successful engraftment and development of human T cells, 1×10^7 WT1-expressing HLA-A*02⁺ SKM-1 tumor cells were subcutaneously inoculated. After 7 days, when tumor size reached an average volume of 150 mm³, mice received weekly administrations of 1 mg/kg WT1-TCB or histidine buffer (vehicle) for 6 weeks. The experimental study protocol was reviewed and approved by local government authorities (2011-128).

In vivo study with AML patient-derived xenograft cells

NSG mice were engrafted with patient-derived xenograft (PDX) cells expressing enhanced firefly luciferase, and tumor burden was monitored by bioluminescence imaging as previously described.⁴⁸ After successful engraftment, HD T cells were transplanted, followed by weekly administration of 3 mg/kg WT1-TCB or Ctrl-TCB beginning on day 30. One WT1-TCB-treated mouse died during imaging on day 32. The experimental study protocol was reviewed and approved by local government authorities (ROB-55.2-2532.Vet_02-20-159).

Results

Quantitative PCR shows WT1 is expressed in >90% of AML samples at initial diagnosis and at relapse

We analyzed WT1 expression levels in PBMCs of 112 patients with AML by using quantitative real-time PCR at initial diagnosis, in remission, and at time of relapse or in refractory patients (Figure 1A). WT1 expression, defined as >10 WT1 copies per 10⁴ copies of ABL, was observed in 59 of 65 AML patient samples taken at the time of initial diagnosis.⁴⁹ Moreover, WT1 expression levels correlated with the percentage of AML blasts: expression was observed in 2 of 26 samples taken at the time of complete remission with a blast percentage <5%. Conversely, upon relapse or in refractory disease, WT1 was expressed in 17 of 21 cases. Furthermore, WT1 expression was observed in 79% (n = 38) of cancer cell lines (Figure 1B).

Similarly, WT1 expression in bone marrow samples correlated to the percentage of blasts (Figure 1C). WT1 expression was observed in 35 of 38 samples taken at primary diagnosis. In posttherapy samples, WT1 expression was detected in 1 of 8 cases in which the blast percentage was <5%. On the contrary, 10 of 16 samples were WT1 positive if the blast percentage exceeded 5% as a result of relapsed or refractory disease.

The WT1 expression level (mean \pm standard error of the mean [SEM]) tended to be higher for NPM1 mutant samples compared with wild-type (1055 \pm 251 vs 985 \pm 429 WT1 copies/10⁴ ABL copies; $P = .1$) and was higher in samples with mutated FLT3-ITD (2155 \pm 922 vs 582 \pm 103 WT1 copies/10⁴ ABL copies; $P < .05$) and lower in CEBPA mutant samples (92 \pm 43 vs 1299 \pm 482 WT1 copies/10⁴ ABL copies; $P < .005$) (Figure 1D).

Specific binding to WT1_{RMF}-pMHC complexes

For the work presented here, trivalent 2 + 1 IgG TCB antibodies were generated with bivalent recognition of the WT1_{RMF}-pMHC complex and monovalency for the CD3 ϵ chain of the TCR (Figure 2A). The monovalent affinities of WT1-TCB for CD3 ϵ and WT1-pMHC as determined by surface plasmon resonance are shown in Table 1.

Alanine scanning revealed the key amino acids required for binding of the RMF peptide (Figure 2B; supplemental Figure 2A-B). These data were confirmed by using a novel peptide-MHC array in which the binding contribution of each amino acid can be investigated by replacement of the remaining amino acids (Figure 2C; supplemental Figure 2C). Both methods showed that apart from the anchor residues Met2 and Leu9, the residues Arg1, Phe3, Asn5, and Ala6 are particularly important for recognition of the

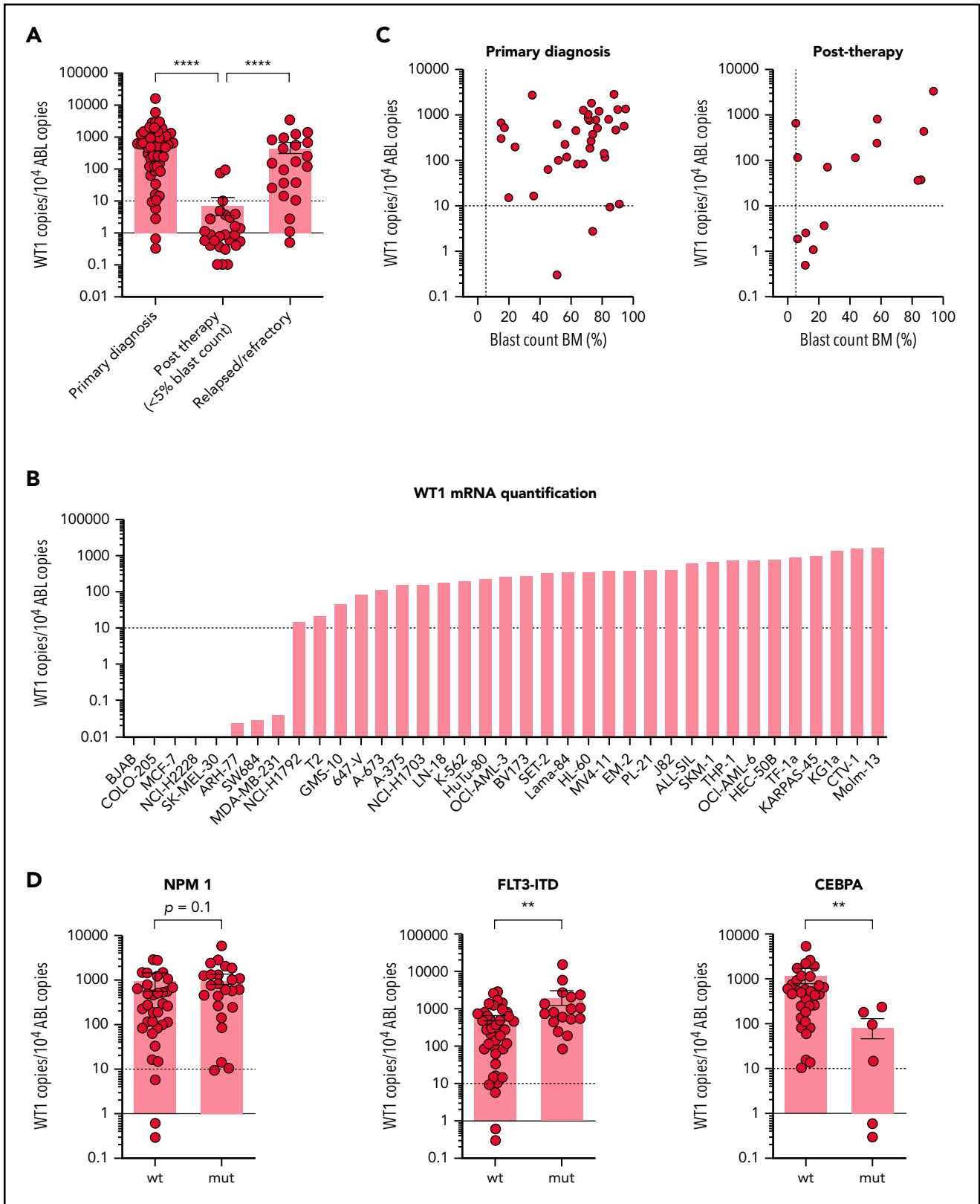


Figure 1. Analysis of WT1 expression in primary AML cells and tumor cell lines by real-time qPCR. (A) WT1 expression in primary AML cells at different time points during the course of the disease (primary diagnosis, $n = 65$; posttherapy, $n = 26$; relapsed/refractory, $n = 21$). (B) WT1 expression in tumor cell lines ($n = 37$). (C) Correlation of blast count and WT1 expression in bone marrow (BM) samples of patients with AML at primary diagnosis ($n = 38$) and posttherapy ($n = 24$). (D) Correlation of WT1 expression and NPM1 (wild-type [wt], $n = 37$; mutant [mut], $n = 25$), FLT3-ITD (wt, $n = 45$; mut, $n = 17$), and CEBPA (wt, $n = 34$; mut, $n = 6$) mutational status. Bars represent mean \pm SEM. Statistical analysis: Mann-Whitney U test. ** $P < .01$, **** $P < .0001$.

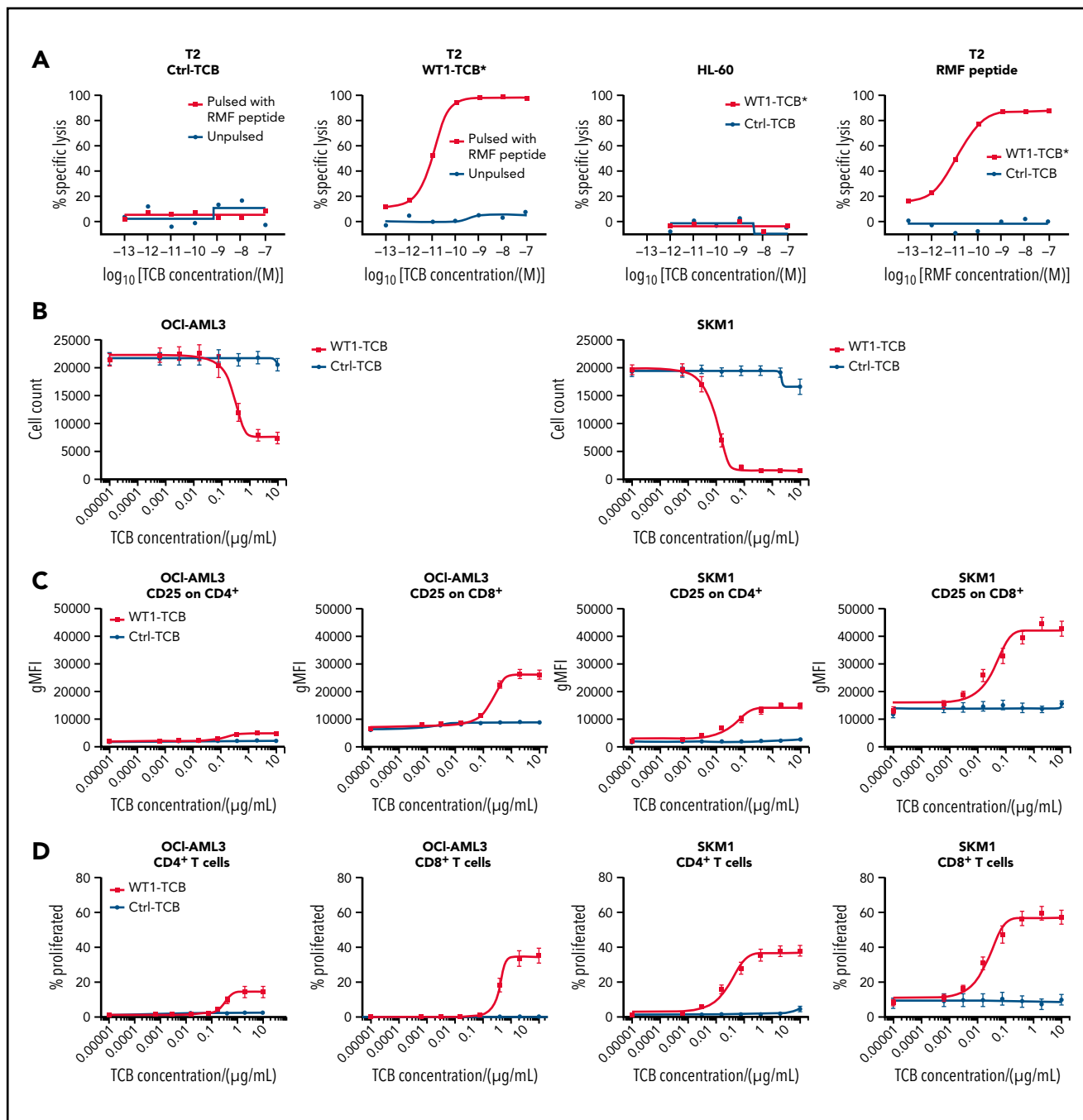


Figure 3. Dose–response relationship after treatment with WT1-TCB in cocultures of tumor cell lines with HD T cells. (A) Transporter associated with antigen processing–deficient HLA-A*02⁺ T2 cells, unpulsed (black) vs RMF peptide pulsed (red) after treatment with Ctrl-TCB (left) or WT1-TCB* (second from left). Second from right: control with HLA-A02[−] HL-60 cells and Ctrl-TCB (black) or WT1-TCB* (red). Right: T2 cells pulsed with increasing doses of RMF peptide and treatment with 10^{−8} M Ctrl-TCB (black) or WT1-TCB* (red). (B) Killing assay performed on AML cell lines (OCI-AML3 and SKM-1) and treated with varying concentrations of WT1-TCB (red) or Ctrl-TCB (black). Tumor cell killing was evaluated after 44 hours (SKM-1) or 68 hours (OCI-AML3); n = 10. (C) CD25 expression (C) and proliferation of CD4⁺ and CD8⁺ T cells (D) after 3 days in killing assays using AML cell lines (OCI-AML3 and SKM-1) at varying concentrations of WT1-TCB (red) or Ctrl-TCB (black); n = 6. gMFI, geometric mean fluorescence intensity.

RMF–pMHC complex by 11D06, whereas residues Pro4, Pro7, and Tyr8 are less critical for binding.

The X-ray structure of the HLA-A*02/RMF–pMHC complex bound by the 11D06 Fab fragment, resolved at 2.64 Å (pdb code 7BBG), allowed a closer examination of the binding motif compared with the known crystal structure of the ESK1 antibody (Figure 2D-E).³⁴ The structure shows that the Fab 11D06 bound to MHC by

contributions of all complementarity-determining regions. The RMF–pMHC–11D06 complex is characterized by a contact surface area of ~397 Å² in the center of the pMHC complex, which corresponds to a peptide contribution of ~107 Å² (27%); for the ESK1 antibody, the contact surface area is ~505 Å² with a peptide contribution of ~60 Å² (12%) that is shifted to the N terminus.³⁷ ESK1 binds HLA via Arg1 of the RMF peptide, whereas 11D06 interacts with the central bulge of the peptide, mainly through

Table 2. Summary of cell line killing mediated by WT1-TCB

Cell line	Disease of tissue origin	WT1 mRNA	HLA-A typing based on TRON database	Time of EC ₅₀ evaluation (h)	EC ₅₀ (nM) T-cell killing in vitro	EC ₅₀ (μg/mL) T-cell killing in vitro
SKM-1	AML	+	33:03, 02:07	44	0.16-1.25	0.032-0.25
OCI-M1	AML	+	03:01, 02:01	68	0.75-2.15	0.15-0.43
OCI-AML3	AML	+	23:01, 02:01	68	0.20-6.75	0.04-1.35
Set-2	AML	+	33:03, 02:01	48	0.8-7.6	0.16-1.52
COV318	Ovarian carcinoma	+	03:01, 02:01	48	4	0.8
Ovcar-3	Ovarian carcinoma	+	02:01, 29:02	48	10.8	2.16
T98G	Glioblastoma	+	02:01, 02:01	48	0.5	0.1
MDA-MB-231	Breast adenocarcinoma	+	02:01, 02:17	48	0.87	0.174
BV173	Blast phase chronic myelogenous leukemia	+	30:01, 02:01	48	0.97-13.75	0.19-2.75
SW480	Colorectal adenocarcinoma	+	02:01, 24:02	48	0.05-5.4	0.01-1.08
SW620	Colorectal adenocarcinoma	+	02:01, 24:02	48	5.8-8.5	1.16-1.7
HEC-50B	Endometrial adenocarcinoma	+	02:07, 02:07	48	5.95-6.2	1.19-1.24
ARH-77	Plasma cell leukemia	—	02:01, 03:01	NA	NA	NA
HL-60	Promyelocytic leukemia	+	01:01	NA	NA	NA

NA; not applicable.

Asn5. The peptide's central core is arranged similarly to the natural TCR-HLA assemblies, with the CDR3 loops of both chains arranged around the peptide amino acids 4-6. A similar pattern of binding is observed in the complex formed between the affinity-enhanced WT1- $\alpha_7\beta_2$ TCR and A2-RMF (supplemental Figure 3; supplemental Tables 1-3).⁵⁰

Targeted quantification of HLA-A*02 presented WT1_{RMF} peptide using immunoprecipitation combined with mass spectrometry

To provide evidence for RMF peptide presentation on MHC, we developed a novel mass spectrometry-based approach (details are given in the supplemental Data). To test the performance of the method, the RMF peptide was pulsed on T2 cells. The exogenously loaded peptide was recovered and detected with a concentration-dependent signal. Furthermore, the existence of the endogenous peptide on SKM-1 cells was confirmed by its detection, albeit at very low levels (supplemental Figure 4). The workflow has been further optimized for primary AML cells, including immunoprecipitation by WT1-TCB and sample upscaling. Thereby, the endogenous RMF peptide was quantified up to 17 fmol, which is equivalent to 152 copies per cell for AML patient no. 1 (Figure 2F). Patient characteristics are provided in supplemental Table 8.

Antibody binding is dependent on WT1 and HLA-A*02 expression and results in T-cell cytotoxicity against tumor cells

We evaluated the WT1-TCB*-mediated T-cell cytotoxicity by coculturing T cells from HDs with different tumor cell lines.

Flow cytometry measurements showed that WT1-TCB* elicited antibody-mediated T-cell cytotoxicity in cocultures with RMF peptide-pulsed T2 cells in a WT1-TCB and RMF peptide dose-dependent manner. No lysis was observed in cocultures with unpulsed T2 cells, HLA-A*02⁻ WT1⁺ HL-60 cells, or Ctrl-TCB (Figure 3A). Killing of HLA-A*02⁺ tumor cells expressing the RMF peptide from endogenous WT1 protein by WT1-TCB was assessed on a panel of cell lines by counting living target cells or analyzing distinct dead cell protease activity. The most potent killing was observed by using the HLA-A*02:07 cell line SKM-1; other tested HLA-A*02:01 AML cell lines, including OCI-AML3, were killed with lower potency, whereas non-HLA-A*02-expressing cells were not killed (Figure 3B; Table 2).

We also assessed the ability of WT1-TCB to activate and expand T cells by measuring upregulation of CD25 and proliferation of dye-labeled cells. Consistent with the results regarding tumor cell killing, T-cell activation and proliferation were strongest in the SKM-1 cell line and lower with OCI-AML3. In addition, T-cell activation and proliferation were consistently higher for CD8⁺ compared with CD4⁺ T cells (Figure 3C-D).

Finally, we assessed the killing of other HLA-A*02⁺ tumor cell lines that either express or do not express WT1 (based on mRNA values). The killing of non-AML cell lines was not as efficacious as the killing of SKM-1 cells, with 50% effective concentration (EC₅₀) values in most cases being >10-fold higher (Table 2).

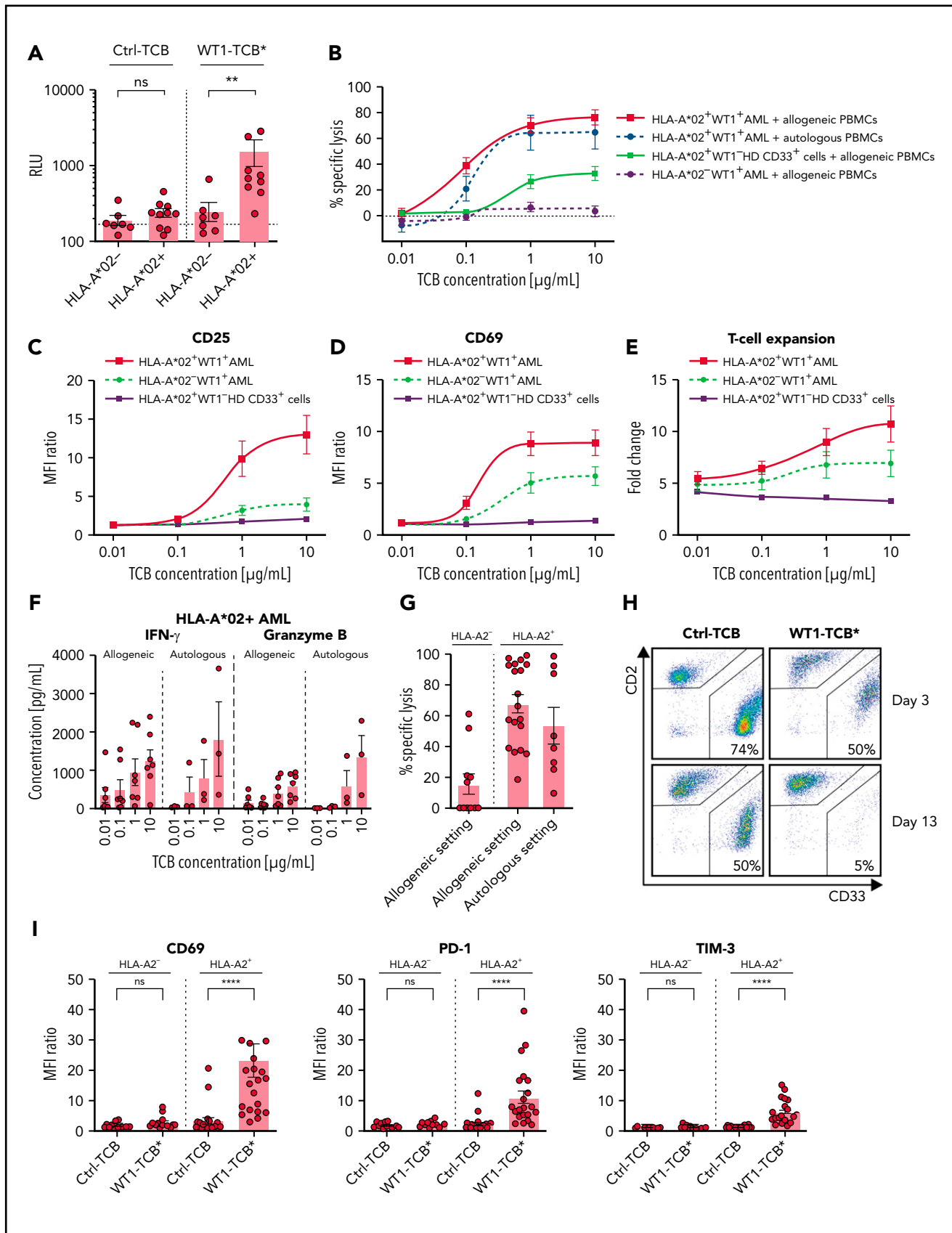


Figure 4. WT1-TCB-mediated T-cell cytotoxicity and T-cell activation. (A) Induction of downstream TCR signaling in NFAT Jurkat Reporter cells upon recognition of RMF peptide–MHC complexes on primary AML cells. Statistical analysis, Mann-Whitney *U* test ($n = 10$). (B) Dose-dependent specific lysis of primary HLA-A*02⁺ AML cells by allogeneic (black solid line; $n = 9$) or autologous (black dashed line; $n = 3$) PBMCs after 48 hours in short-term cytotoxicity assays with WT1-TCB. Controls: HLA-A*02⁺ WT1⁻ CD33⁺ HD cells (gray solid line; $n = 6$) and primary HLA-A*02⁻ AML cells (gray dashed line; $n = 10$). CD25 (C) and CD69 (D) expression on CD3⁺ T cells after 48 hours in

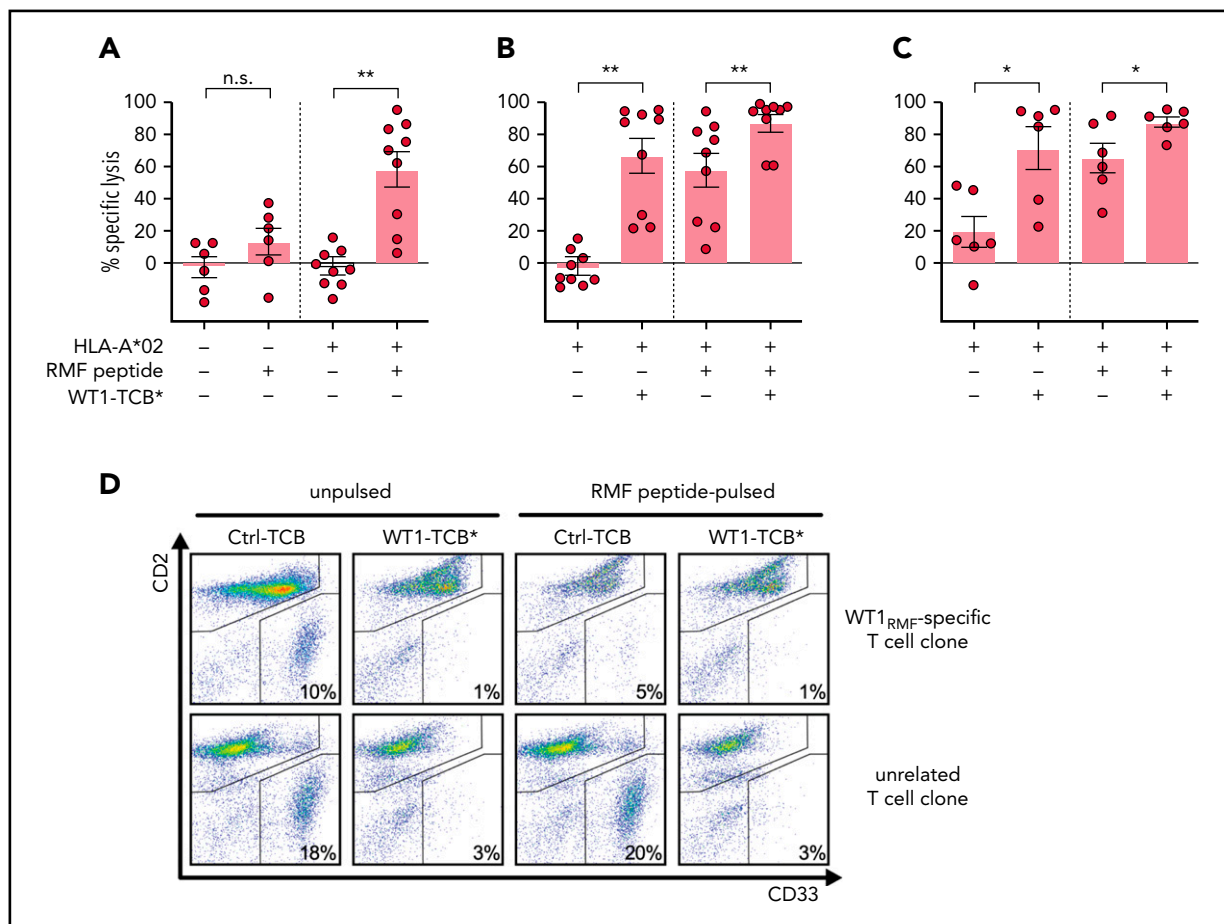


Figure 5. WT1-TCB* vs WT1-specific T cells. (A) Specific lysis of unpulsed and RMF peptide-pulsed primary AML cells from HLA-A*02⁻ and HLA-A*02⁺ patients by WT1_{RMF}-specific T-cell clone after 3 days in feeder layer-based long-term cocultures. Specific lysis was calculated by subtraction of unspecific lysis by HD T cells under the same conditions (n = 6-9). (B) Specific lysis of primary AML cells after 3 days in feeder layer-based long-term cocultures with WT1_{RMF}-specific T-cell clone and treatment with WT1-TCB* compared with HD T cells (n = 9). (C) Specific lysis of primary AML cells (all NPM1 wild-type) after 3 days in feeder layer-based long-term cocultures with WT1_{RMF}-specific T-cell clone and treatment with WT1-TCB*. Specific lysis was calculated by subtraction of unspecific lysis by a T-cell clone targeting an unrelated epitope of mutated NPM1 (n = 6). (D) Representative dot plots from flow cytometry analysis showing CD2 and CD33 expression in lysis experiments. Bars represent mean ± SEM. Statistical analysis: Mann-Whitney U test. *P < .05, **P < .01. n.s., not significant.

Induction of downstream TCR signaling in cocultures with primary AML cells

We monitored downstream TCR signaling by coculturing NFAT Luciferase Reporter Jurkat cells with primary AML cells in the presence of WT1-TCB* (10 nM). WT1-TCB* significantly induced downstream TCR signaling in cocultures with HLA-A*02⁺ primary AML cells but not with cells from HLA-A*02⁻ patients. No signal was observed if the nonspecific Ctrl-TCB was used (Figure 4A). Induction of TCR signaling was dose dependent, with an EC₅₀ of WT1-TCB* of 5.7 nM in HLA-A*02⁺ AML cells (supplemental Figure 5).

Lysis of primary AML cells is dose dependent

We assessed WT1-TCB-mediated cytotoxicity against primary AML cells by autologous or HD PBMCs in conjunction with various concentrations of WT1-TCB. WT1-TCB mediated the killing of

HLA-A*02⁺ AML cells in the allogeneic and autologous settings (mean ± SEM specific lysis after 48 hours with 10 μg/mL TCB, 76.6 ± 5.9% and 64.7 ± 12.4%; n = 9 and 3, respectively). Lysis of AML cells was dose dependent, with an EC₅₀ value of ~0.1 μg/mL (0.5 nM) for both settings. Conversely, no lysis of HLA-A*02⁻ AML cells was observed, and only low levels of lysis in HD-derived HLA-A*02⁺ WT1⁻ myeloid cells were recorded (Figure 4B). Correspondingly, using HLA-A*02⁺ AML cells, we observed dose-dependent T-cell activation, expansion, interferon-γ secretion, and granzyme B secretion (Figure 4C-F).

T-cell cytotoxicity against primary AML cells ex vivo

To further support the potency of WT1-TCB* against primary AML cells, we cocultured primary AML cells with HD or autologous

Figure 4 (continued) killing assays with allogeneic PBMCs and primary HLA-A*02⁺ AML cells (black solid line; n = 9), primary HLA-A*02⁻ AML cells (gray dashed line; n = 10), or HLA-A*02⁺ WT1⁻ CD33⁺ HD cells (gray solid line; n = 6). (E) T-cell proliferation after 96 hours in killing assays with allogeneic PBMCs and primary HLA-A*02⁺ AML cells (black solid line; n = 8), primary HLA-A*02⁻ AML cells (gray dashed line; n = 7), or HLA-A*02⁺ WT1⁻ CD33⁺ HD cells (gray solid line; n = 3). (F) Secretion of interferon-γ (IFN-γ) and granzyme B in allogeneic and autologous settings after 72 hours in a short-term cytotoxicity assay with primary HLA-A*02 AML cells. (G) Specific lysis of primary AML cells by allogeneic T cells (left: HLA-A*02⁻ AML, n = 11; center: HLA-A*02⁺ AML, n = 19) or autologous T cells (right: HLA-A*02⁺ AML, n = 8) after 10 to 13 days in long-term cocultures and treatment with WT1-TCB*. (H) Representative dot plots from flow cytometry analysis showing CD2 and CD33 expression in long-term coculture samples. (I) Upregulation of activation and surrogate exhaustion markers on CD33⁺ T cells on days 3 to 4 in long-term cocultures with primary HLA-A*02⁺ and HLA-A*02⁻ AML cells (n = 14-22). Bars represent the mean ± SEM. Statistical analysis: Kruskal-Wallis test and subsequent Dunn's test. **P < .01, ****P < .0001. MFI, mean fluorescence intensity; n.s., not significant; RLU, relative luminescence units.

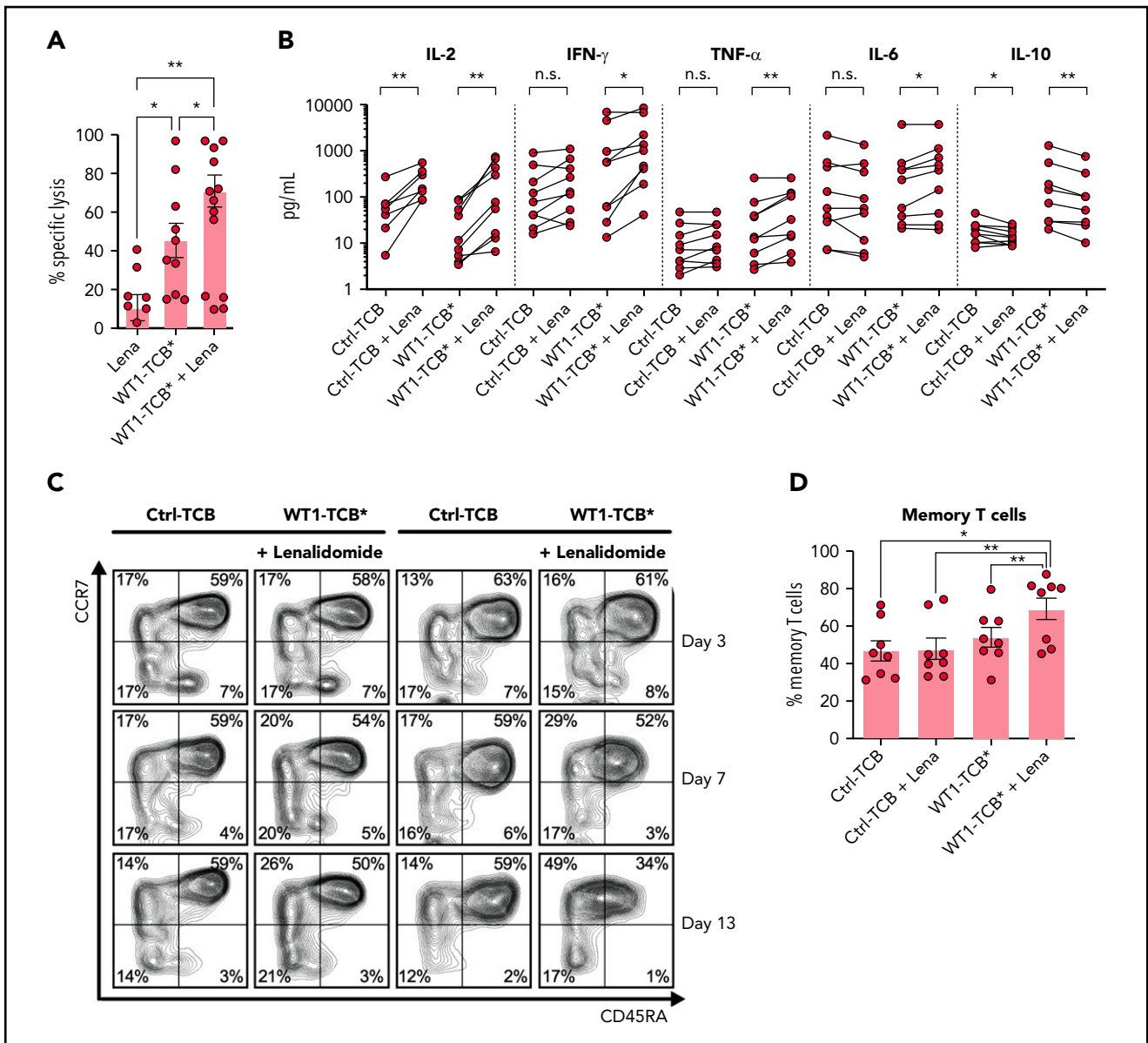


Figure 6. WT1-TCB*-mediated cytotoxicity in combination with lenalidomide (Lena). (A) WT1-TCB*-mediated specific lysis of primary AML cells significantly increased in combination with Lena after 4 days of coculture with HD T cells ($n = 9-10$). Lena was added at a concentration of $10 \mu\text{M}$ together with 10 nM WT1-TCB* in ex vivo cytotoxicity assays with primary AML cells and HD T cells at an E:T ratio of 1:2 for 4 days. (B) Levels of proinflammatory cytokines increase after combination of WT1-TCB* with Lena and levels of the anti-inflammatory interleukin 10 (IL-10) decrease ($n = 9$). (C) Representative example of CD45RA and CCR7 expression analysis. (D) Percentages of central memory T cells after 7 to 10 days of treatment ($n = 8$). Bars represent the mean \pm SEM. Statistical analysis: Wilcoxon matched-pairs signed-rank test. * $P < .05$, ** $P < .01$. n.s., not significant; TNF- α , tumor necrosis factor α .

T cells in a feeder layer-based long-term culture system. This action enabled us to assess the specific lysis of AML cells over a therapeutically relevant time frame. WT1-TCB* induced specific cytotoxicity of primary HLA-A*02⁺ AML cells upon addition of allogeneic T cells from HDs (mean \pm SEM specific lysis, $67 \pm 6\%$ after 13-14 days; $n = 19$). WT1-TCB* also mediated the killing of primary AML cells in an autologous setting (mean \pm SEM specific lysis, $54 \pm 12\%$ after 11-14 days; $n = 8$). HLA-A*02⁻ AML cells were not significantly killed (Figure 4G-H). Corresponding upregulation of T-cell activation and checkpoint molecules was only observed with HLA-A*02⁺ AML cells (mean \pm SEM fluorescence intensity fold change: CD69, 9.3 ± 1.5 ; PD-1, 5.1 ± 0.7 ; TIM-3, 4.7 ± 0.6 ; $n = 22$) (Figure 4I).

Lysis of healthy, bone marrow-derived CD34⁺ cells is low

To evaluate on-target off-leukemia WT1-TCB*-mediated cytotoxicity against healthy HLA-A*02⁺ bone marrow cells, we prepared cocultures with autologous T cells and varying concentrations of WT1-TCB. Specific lysis of CD34⁺ cells was observed in a dose-dependent manner at 48 hours, and the EC₅₀ value was $0.15 \mu\text{g/mL}$. The effect was minimal at $0.1 \mu\text{g/mL}$ (mean \pm SEM specific lysis, $8.3 \pm 3.3\%$; $n = 8$) (supplemental Figure 6A) and increased to $34.2 \pm 9.0\%$ at $1 \mu\text{g/mL}$. Expression of the activation marker CD69 was low after 24 hours in the presence of WT1-TCB at concentrations equal to the EC₅₀ value or lower (mean \pm SEM fluorescence

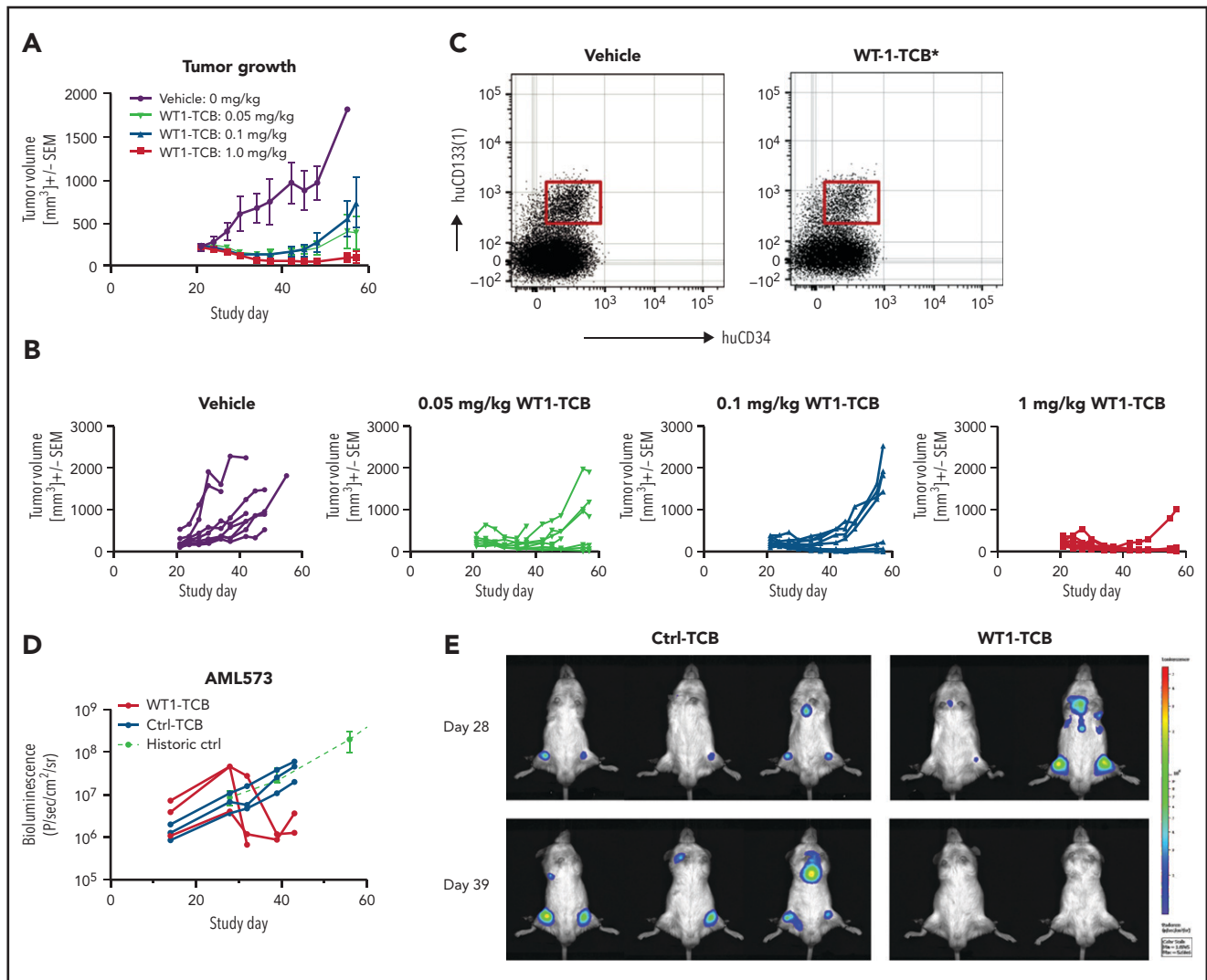


Figure 7. Antitumor efficacy of WT1-TCB in humanized mouse models. (A-B) Tumor growth curves of the SKM-1 model in hSC-NSG mice treated once weekly with vehicle control or 0.05, 0.1, or 1 mg/kg of WT1-TCB. (C) Cytometric analysis of the CD34⁺CD133⁺ stem cell population in the bone marrow of SKM-1 tumor-bearing hSC-NSG mice engrafted with cord blood from HLA-A*02⁺ donors after 54 days of treatment with WT1-TCB*. (D-E) Tumor growth in AML PDX mice (AML573) treated once weekly with 3 mg/kg WT1-TCB or Ctrl-TCB beginning on day 30, assessed by in vivo imaging. One WT1-TCB-treated mouse died during imaging on day 32.

intensity ratio, 62.4 ± 39.0 ; $n = 8$; $0.1 \mu\text{g/mL}$ TCB). Pulsing with the RMF peptide exacerbated the lysis of CD34⁺ cells at all concentrations and increased T-cell activation (supplemental Figure 6B). To further validate the absence of negative effects on healthy hematopoiesis, we performed colony-forming unit assays with HD bone marrow cells. No difference in colony formation was observed for samples treated for 48 hours with either 0.1 or $2 \mu\text{g/mL}$ WT1-TCB compared with Ctrl-TCB ($n = 3$ and 1 , respectively) (supplemental Figure 6C).

The cytotoxicity against AML cells is higher compared with a WT1_{RMF}-specific T-cell clone

We compared the cytotoxicity of T cells mediated by WT1-TCB* vs that of a WT1_{RMF}-specific T-cell clone isolated from HDs by streptamer technology.⁵¹ A WT1_{RMF}-specific T-cell clone was cocultured with primary AML cells for 3 days in a feeder layer-based long-term culture system with or without

WT1-TCB*. To determine the extent of nonspecific background lysis, we prepared additional control samples with HD T cells or an unrelated T-cell clone without addition of WT1-TCB*. Specific lysis was calculated relative to these controls.

No specific lysis of HLA-A*02⁻ primary AML cells by WT1_{RMF}-specific T-cell clone was observed. Surprisingly, specific lysis against HLA-A*02⁺ primary AML cells was only observed after we loaded target cells with RMF peptide (mean \pm SEM specific lysis, $-3 \pm 4\%$ [unpulsed]; $58 \pm 11\%$ [pulsed]; $n = 9$) (Figure 5A). Conversely, addition of WT1-TCB* induced specific lysis of HLA-A*02⁺ primary AML cells also without RMF peptide loading (mean \pm SEM specific lysis, $67 \pm 11\%$ [unpulsed], $88 \pm 5\%$ [pulsed]; $n = 9$) (Figure 5B). Similar results were obtained by using an unrelated T-cell clone as a reference instead of HD T cells (mean \pm SEM specific lysis, $71 \pm 13\%$ [unpulsed]; $88 \pm 3\%$ [pulsed]; $n = 6$) (Figure 5C-D).

Lenalidomide enhances cytotoxicity against primary AML cells

The addition of lenalidomide (AbMole BioScience, Brussels, Belgium) enhanced WT1-TCB*-mediated T-cell cytotoxicity in cocultures of primary AML cells and HD T cells (mean \pm SEM specific lysis on days 3-4, $45.4 \pm 9.0\%$ vs $70.8 \pm 8.3\%$; $P = .015$; $n = 9-10$) (Figure 6A). Similarly, addition of lenalidomide with WT1-TCB* increased the secretion of pro-inflammatory cytokines and reduced levels of IL-10 (Figure 6B). Furthermore, combination with lenalidomide promoted the differentiation of naive T cells toward a memory phenotype characterized by downregulation of CD45RA (Figure 6C-D).

Tumor growth inhibition in in vivo mouse models

We assessed the pharmacokinetic parameters of WT1-TCB in a human FcRn transgenic mouse model and observed a mean terminal elimination half-life of 10.7 days (supplemental Figure 7). Next, we evaluated the antitumor activity of WT1-TCB in a SKM-1 xenograft model in NSG mice engrafted with human stem cells (hSC-NSG). We tested doses of 0.05, 0.1, and 1 mg/kg WT1-TCB* administered once weekly and observed a dose-dependent efficacy (Figure 7A-B).

Notably, WT1-TCB* treatment did not result in adverse effects on CD34⁺ hSCs when tested in hSC-NSG mice engrafted with HLA-A*02⁺ stem cells (Figure 7C). Although WT1-TCB* mediated potent antitumor efficacy at concentrations of 1 and 10 mg/kg, it did not induce signs of weight loss or depletion of CD34⁺ stem cells in the bone marrow of hSC-NSG mice at day 57. This supports the in vivo specificity of WT1-TCB* (based on the 11D06 binder) in a system expressing HLA-A*02 on hSCs and in the derived cell lineages in blood, bone marrow, and lymphoid tissues.

In addition, antitumor activity of WT1-TCB was seen in an AML PDX model. We observed a reduction of the tumor burden after weekly administration of WT1-TCB compared with Ctrl-TCB, as assessed by in vivo imaging (Figure 7D-E). In a second experiment using a different PDX model, WT1-TCB-treated mice had a reduced number of human CD45⁺CD33⁺ cells in spleen and bone marrow compared with Ctrl-TCB-treated mice after 10 days of treatment (supplemental Figure 8).

Discussion

The current study evaluated a novel 2 + 1 TCB antibody construct that targets an epitope of the intracellular antigen WT1 in the context of HLA-A*02. WT1 is overexpressed in a number of tumor entities, including AML, and is thus a universal target antigen in immunotherapeutic strategies. It has been extensively described as a leukemia-associated antigen with a disease-restricted expression profile.^{22,23} Analysis of WT1 expression in bone marrow sampled from patients with AML during the course of the disease revealed a strong correlation between the percentage of leukemic blasts in the bone marrow and the number of copies of WT1 mRNA. Accordingly, WT1 has been used as a prognostic marker for assessing minimal residual disease.^{49,52-55} The recurrence of WT1 expression at time of relapse supports the hypothesis that WT1 plays a pathophysiological role in leukemic cell survival. Several in vitro studies have shown the modulation of leukemic

cell growth by upregulation and downregulation of WT1; however, the precise role of WT1 in leukemia remains elusive.⁵⁶⁻⁵⁸

WT1-TCB was designed to specifically recognize the WT1-derived RMF peptide in the context of HLA-A*02. Alanine scanning and a novel peptide MHC array method showed that 6 of the 9 residues of the RMF peptide are important for binding WT1-TCB. A TCR-mimicking antibody targeting the same epitope, named ESK1, has been reported.^{34,35,59,60} However, this antibody has not entered clinical development, most likely owing to off-target binding, as epitope binding of ESK1 relies almost exclusively on peptide residue Arg1, allowing recognition of several other self peptides.³⁷ X-ray crystallography of the RMF-pMHC complex bound to the WT1-TCB Fab fragment further revealed a considerably higher contribution of the RMF peptide to the overall contact surface area compared with ESK1.^{37,50}

The confirmation that the RMF peptide is presented as part of a pMHC complex relies on cellular data, but so far the RMF peptide could not be extracted from cancer cells.^{61,62} By developing a novel mass spectrometry-based approach, we provide qualitative evidence for endogenous RMF peptide presentation using SKM-1 cells. Further optimization, including immunoprecipitation by WT1-TCB, allowed the first quantification of endogenous RMF peptide presentation on an AML patient sample. This provides evidence that HLA-A*02/RMF-pMHC complexes are presented on primary AML cells at a reasonable density and also shows the selectivity of WT1-TCB toward this complex.

In short-term cytotoxicity experiments, we observed the dose-dependent WT1-TCB-mediated lysis of primary AML cells, underlining that endogenous RMF peptide is presented. Using our pre-established ex vivo long-term culture system for AML cells,⁴⁷ we observed WT1-TCB-mediated cytotoxicity against primary AML cells by allogeneic and autologous T cells over a therapeutically relevant time frame. Interestingly, cytotoxicity was higher in the allogeneic setting, which supports previous findings on T-cell dysfunction in AML.^{63,64} Importantly, our in vitro findings were supported by our in vivo demonstration of tumor growth inhibition by WT1-TCB using different AML PDX models and a SKM-1-xenograft model. In the latter model, some animals exhibited tumor progression after initial tumor control. In an RNA-sequencing analysis of the possible escape mechanisms, we did not observe downregulation of WT1, in contrast to HLA-A*02; however, this was not the case in all samples.

Because low frequency of WT1 RNA-expressing hSCs has been reported,²¹ we evaluated WT1-TCB-mediated on-target, off-leukemia cytotoxicity against HD CD34⁺ bone marrow cells. We observed only low WT1-TCB-mediated target cell lysis and T-cell activation and did not observe killing of CD34⁺ hSCs in the humanized NSG mouse model. This indicates that the RMF peptide is not presented on the surface of HLA-A*02⁺ healthy CD34⁺ cells to an extent that WT1-TCB initiates T-cell activation. This observation is consistent with results from a clinical trial with WT1_{RMF}-TCR transgenic T cells that reported no corresponding adverse events.²⁹

Target antigen recognition by WT1-TCB mimics the physiological MHC-TCR interaction but differs by bivalent vs monovalent binding. WT1-TCB mediated the lysis of unpulsed and RMF peptide-pulsed primary AML cells, whereas a WT1_{RMF}-specific

T-cell clone mediated the killing of only peptide-pulsed target cells. One explanation for these findings is that the 2 + 1 molecular format confers higher avidity (double-digit nanomolar affinity for the pMHC complex as opposed to the micromolar affinity that is typical for TCRs), thus enabling target cell lysis even if only low numbers of pMHC complexes are presented. The TCR affinities for nonmutated self peptides such as WT1 have been shown to be lower than those for foreign antigens, which also impedes the generation of high-affinity TCR transgenic T cells for adoptive transfer. Nevertheless, the adoptive transfer of WT1-specific T cells or TCR transgenic T cells has exhibited antileukemic activity in clinical trials.^{27,29} Recently, WT1_{RMF}-TCR transgenic T cells were reported to prevent AML relapse in a small cohort of patients after hematopoietic cell transplantation, providing proof-of-concept for targeting WT1.²⁹

To further augment cytotoxicity, we evaluated the combination of WT1-TCB with lenalidomide, a drug that has been shown to have a stimulatory effect on T cells.^{65,66} We observed a significant increase of specific cytotoxicity and levels of pro-inflammatory cytokines, as well as a shift in the T-cell compartment toward the memory phenotype. The latter is likely a secondary effect due to increased secretion of interl-2, resulting in increased T-cell proliferation and activation. Our observations are consistent with results from other trials of lenalidomide combinations, underlining the rationale behind this combinatorial approach.⁶⁷⁻⁶⁹

In summary, we showed that WT1-TCB facilitates potent *in vitro*, *ex vivo*, and *in vivo* killing of AML cell lines and primary AML cells. These properties led to the initiation of an entry-into-human clinical trial (#NCT04580121) for the treatment of relapsed/refractory AML.

Acknowledgments

The authors thank Sabine Sandner-Thiede, Marina Leeping, Elke Habben, Ewelina Zientara, Sabine Reinkunz, and Anne-Sophie Neumann (University Hospital, LMU Munich) for their excellent technical support. They thank Christoph Lampert and Victor Levitsky (both previously with Roche) for the initial experiments on precursors of WT1-TCB. Thanks also go to Elfriede Nößner and Andreas Moosmann for their expert advice. The authors also acknowledge the iFlow Core Facility of the University Hospital, LMU Munich (INST 409/225-1 FUGG) for assistance with the generation of flow cytometry data.

The work was supported by a German Research Council (DFG) grant provided within the Sonderforschungsbereich SFB 1243 (K.S.; I.J.) and research grant SU197/3-1 (application number 451580403, M. Subklewe), the Bavarian Elite Graduate School "i-target" (M.R.), the Wilhelm-Sander Stiftung (project number 2018.087.1, G.H.) and the European Research Council (Consolidator Grant 681524 [I.J.]). L.V. acknowledges support by the Italian Ministry of Health (RF-2011-02348034 and TRANSCAN HLALOSS), by the Associazione Italiana per la Ricerca sul Cancro (Start-Up Grant 14162), and by the DKMS

Mechtild Harf Foundation (DKMS Mechtild Harf Research Grant 2015). This study was supported, in part, by research funding from Roche to M.S.

Authorship

Contribution: C. Klein, W.X., P.U., and M. Subklewe designed the study and supervised the project; C.A., C. Klein, V.P., G.H., M. Subklewe, M.v.B.-B., and F.S.L. wrote the manuscript; C.A., G.H., V.P., L.J.H., A.A., J.C., K.H., P.E.R., A.S., J.S., E.L., A.D., D.O.-F., J.B., A.B., C.G., A.C., V.L., and J.P. performed the experiments and analyzed and/or interpreted the data; M. Subklewe, W.X., C. Krupka, M.R., F.S.L., L.V., B.V., I.J., E.M.-B., and A.-C.W. were involved in research design and data interpretation; N.K. and K.S. performed the real-time qPCR analyses; A.T. and M. Schmitz generated and provided the WT1-specific T-cell clones; and A.B. and J.B. determined and analyzed the crystal structure.

Conflict-of-interest disclosure: C. Klein, L.J.H., J.S., V.P., A.S., J.C., and P.U. are, and W.X. was, employed at the Roche Innovation Center Zurich. F.S.L., A.C., A.B., and C.G. are, and C. Krupka was, employed at the Roche Innovation Center Munich, and E.M.-B., A.-C.W., A.D., J.B. A.A., E.L., and D.O.-F. are employed at the Roche Innovation Center Basel. V.L. and J.P. were employed at Roche NimbleGen. These authors also declare patents and ownership of Roche stock. M. Subklewe has received industry research support from Amgen, Gilead, Miltenyi Biotec, MorphoSys, Roche, and Seattle Genetics; has served as a consultant/advisor to Amgen, BMS, Celgene, Gilead, Pfizer, Novartis, and Roche; sits on the advisory boards of Amgen, Celgene, Gilead, Janssen, Novartis, Pfizer, and Seattle Genetics; and serves on the speakers bureau at Amgen, Celgene, Gilead, Janssen, and Pfizer. The remaining authors declare no competing financial interests.

ORCID profiles: C.A., 0000-0001-7924-2042; G.H., 0000-0003-4685-6499; A.D., 0000-0003-1251-8520; D.O.-F., 0000-0002-8783-1960; A.-C.W., 0000-0002-2177-545X; A.B., 0000-0001-5052-0221; K.S., 0000-0002-5139-4957; L.V., 0000-0003-4247-3175; I.J., 0000-0003-1773-7677; M. Subklewe, 0000-0003-3905-0251.

Correspondence: Christian Klein, Roche Pharma Research & Early Development, Roche Innovation Center Zurich, Schlieren, Switzerland; e-mail: christian.klein.ck1@roche.com; or Marion Subklewe, Department of Medicine III, University Hospital, LMU Munich, Munich, Germany; e-mail: marion.subklewe@med.uni-muenchen.de.

Footnotes

Submitted 22 December 2020; accepted 1 July 2021; prepublished online on *Blood* First Edition 19 July 2021. DOI 10.1182/blood.2020010477.

*C.A. and G.H. contributed equally to this study.

The online version of this article contains a data supplement.

There is a *Blood* Commentary on this article in this issue.

The publication costs of this article were defrayed in part by page charge payment. Therefore, and solely to indicate this fact, this article is hereby marked "advertisement" in accordance with 18 USC section 1734.

REFERENCES

- Krishnamurthy A, Jimeno A. Bispecific antibodies for cancer therapy: a review. *Pharmacol Ther*. 2018;185:122-134.
- Sedykh SE, Prinz VV, Buneva VN, Nevinsky GA. Bispecific antibodies: design, therapy, perspectives. *Drug Des Devel Ther*. 2018;12:195-208.
- Abramson R. Overview of targeted therapies for cancer: My Cancer Genome. Available at: <https://www.mycancergenome.org/content/molecular-medicine/overview-of-targeted-therapies-for-cancer>. Accessed 19 December 2020.
- Husain B, Ellerman D. Expanding the boundaries of biotherapeutics with bispecific antibodies. *BioDrugs*. 2018;32(5):441-464.
- Suurs FV, Lub-de Hooge MN, de Vries EGE, de Groot DJA. A review of bispecific antibodies and antibody constructs in oncology and clinical challenges. *Pharmacol Ther*. 2019;201:103-119.
- Topp MS, Gökbuget N, Stein AS, et al. Safety and activity of blinatumomab for adult patients with relapsed or refractory B-precursor acute lymphoblastic

- leukaemia: a multicentre, single-arm, phase 2 study. *Lancet Oncol.* 2015;16(1):57-66.
7. Kantarjian H, Stein A, Gökbuget N, et al. Blinatumomab versus chemotherapy for advanced acute lymphoblastic leukemia. *N Engl J Med.* 2017;376(9):836-847.
 8. Pishvaian M, Morse MA, McDevitt J, et al. Phase 1 dose escalation study of MEDI-565, a bispecific T-cell engager that targets human carcinoembryonic antigen, in patients with advanced gastrointestinal adenocarcinomas. *Clin Colorectal Cancer.* 2016;15(4):345-351.
 9. Ravandi F, Stein AS, Kantarjian HM, et al. A phase 1 first-in-human study of AMG 330, an anti-CD33 bispecific T-cell engager (BiTEs®) antibody construct, in relapsed/refractory acute myeloid leukemia (R/R AML). *Blood.* 2018;132(suppl 1):25.
 10. Hiemstra IH, Engelberts PJ, de Jong B, et al. Duobody-CD3xCD20 shows unique and potent preclinical anti-tumor activity in vitro and in vivo, and is being evaluated clinically in patients with b-cell malignancies. *Blood.* 2018;132(suppl 1):1664LP.
 11. Kebenko M, Goebeler ME, Wolf M, et al. A multicenter phase 1 study of solitomab (MT110, AMG 110), a bispecific EpCAM/CD3 T-cell engager (BiTE®) antibody construct, in patients with refractory solid tumors. *Oncol Immunology.* 2018;7(8):e1450710.
 12. Hipp S, Tai YT, Blanset D, et al. A novel BCMA/CD3 bispecific T-cell engager for the treatment of multiple myeloma induces selective lysis in vitro and in vivo [published correction appears in *Leukemia.* 2017;31(10):2278]. *Leukemia.* 2017;31(8):1743-1751.
 13. Uy GL, Godwin J, Rettig MP, et al. Preliminary results of a phase 1 study of flotetuzumab, a CD123 x CD3 Bispecific Dart® Protein, in patients with relapsed/refractory acute myeloid leukemia and myelodysplastic syndrome. *Blood.* 2017;130(suppl 1):637.
 14. Yuraszek T, Kasichayanula S, Benjamin JE. Translation and clinical development of bispecific t-cell engaging antibodies for cancer treatment. *Clin Pharmacol Ther.* 2017;101(5):634-645.
 15. Tabernero J, Melero I, Ros W, et al. Phase Ia and Ib studies of the novel carcinoembryonic antigen (CEA) T-cell bispecific (CEA CD3 TCB) antibody as a single agent and in combination with atezolizumab: Preliminary efficacy and safety in patients with metastatic colorectal cancer (mCRC). *J Clin Oncol.* 2017;35(suppl 15):3002.
 16. Viardot A, Bargou R. Bispecific antibodies in haematological malignancies. *Cancer Treat Rev.* 2018;65:87-95.
 17. Daver N, Alotaibi AS, Bücklein V, Subklewe M. T-cell-based immunotherapy of acute myeloid leukemia: current concepts and future developments. *Leukemia.* 2021;35(7):1843-1863.
 18. Chau YY, Hastie ND. The role of Wt1 in regulating mesenchyme in cancer, development, and tissue homeostasis. *Trends Genet.* 2012;28(10):515-524.
 19. Wilm B, Muñoz-Chapuli R. The role of WT1 in embryonic development and normal organ homeostasis. *Methods Mol Biol.* 2016;1467:23-39.
 20. Hastie ND. Wilms' tumour 1 (WT1) in development, homeostasis and disease. *Development.* 2017;144(16):2862-2872.
 21. Hosen N, Sonoda Y, Oji Y, et al. Very low frequencies of human normal CD34+ haematopoietic progenitor cells express the Wilms' tumour gene WT1 at levels similar to those in leukaemia cells. *Br J Haematol.* 2002;116(2):409-420.
 22. Sugiyama H. WT1 (Wilms' tumor gene 1): biology and cancer immunotherapy. *Jpn J Clin Oncol.* 2010;40(5):377-387.
 23. Cheever MA, Allison JP, Ferris AS, et al. The prioritization of cancer antigens: a national cancer institute pilot project for the acceleration of translational research. *Clin Cancer Res.* 2009;15(17):5323-5337.
 24. Oka Y, Tsuboi A, Nakajima H, et al. WT1 peptide vaccine for the treatment of malignancies: its development, recent progress, and future perspectives. In: Yamaguchi Y, ed. *Immunotherapy of Cancer.* 1st ed. Tokyo, Japan: Springer; 2016:159-185.
 25. Oka Y, Elisseeva OA, Tsuboi A, et al. Human cytotoxic T-lymphocyte responses specific for peptides of the wild-type Wilms' tumor gene (WT1) product. *Immunogenetics.* 2000;51(2):99-107.
 26. Gao L, Bellantuono I, Elsässer A, et al. Selective elimination of leukemic CD34(+) progenitor cells by cytotoxic T lymphocytes specific for WT1. *Blood.* 2000;95(7):2198-2203.
 27. Chapuis AG, Ragnarsson GB, Nguyen HN, et al. Transferred WT1-reactive CD8+ T cells can mediate antileukemic activity and persist in post-transplant patients. *Sci Transl Med.* 2013;5(174):174ra27.
 28. Tawara I, Kageyama S, Miyahara Y, et al. Safety and persistence of WT1-specific T-cell receptor gene-transduced lymphocytes in patients with AML and MDS. *Blood.* 2017;130(18):1985-1994.
 29. Chapuis AG, Egan DN, Bar M, et al. T cell receptor gene therapy targeting WT1 prevents acute myeloid leukemia relapse post-transplant. *Nat Med.* 2019;25(7):1064-1072.
 30. Van Tendeloo VF, Van de Velde A, Van Driessche A, et al. Induction of complete and molecular remissions in acute myeloid leukemia by Wilms' tumor 1 antigen-targeted dendritic cell vaccination. *Proc Natl Acad Sci U S A.* 2010;107(31):13824-13829.
 31. Anguille S, Van de Velde AL, Smits EL, et al. Dendritic cell vaccination as postremission treatment to prevent or delay relapse in acute myeloid leukemia. *Blood.* 2017;130(15):1713-1721.
 32. Di Stasi A, Jimenez AM, Minagawa K, Al-Obaidi M, Rezvani K. Review of the results of WT1 peptide vaccination strategies for myelodysplastic syndromes and acute myeloid leukemia from nine different studies. *Front Immunol.* 2015;6:36.
 33. Akahori Y, Wang L, Yoneyama M, et al. Antitumor activity of CAR-T cells targeting the intracellular oncoprotein WT1 can be enhanced by vaccination. *Blood.* 2018;132(11):1134-1145.
 34. Dao T, Yan S, Veomett N, et al. Targeting the intracellular WT1 oncogene product with a therapeutic human antibody. *Sci Transl Med.* 2013;5(176):176ra33.
 35. Dao T, Pankov D, Scott A, et al. Therapeutic bispecific T-cell engager antibody targeting the intracellular oncoprotein WT1. *Nat Biotechnol.* 2015;33(10):1079-1086.
 36. Rafiq S, Purdon TJ, Daniyan AF, et al. Optimized T-cell receptor-mimic chimeric antigen receptor T cells directed toward the intracellular Wilms tumor 1 antigen. *Leukemia.* 2017;31(8):1788-1797.
 37. Ataie N, Xiang J, Cheng N, et al. Structure of a TCR mimic antibody with target predicts pharmacogenetics. *J Mol Biol.* 2016;428(1):194-205.
 38. Klein C, Schaefer W, Regula JT, et al. Engineering therapeutic bispecific antibodies using CrossMab technology. *Methods.* 2019;154:21-31.
 39. Regula JT, Imhof-Jung S, Mølhøj M, et al. Variable heavy-variable light domain and Fab-arm CrossMabs with charged residue exchanges to enforce correct light chain assembly. *Protein Eng Des Sel.* 2018;31(7-8):289-299.
 40. Schaefer W, Regula JT, Böhner M, et al. Immunoglobulin domain crossover as a generic approach for the production of bispecific IgG antibodies. *Proc Natl Acad Sci U S A.* 2011;108(27):11187-11192.
 41. Bacac M, Fauti T, Sam J, et al. A novel carcinoembryonic antigen T-cell bispecific antibody (CEA TCB) for the treatment of solid tumors. *Clin Cancer Res.* 2016;22(13):3286-3297.
 42. Silacci M, Brack S, Schirru G, et al. Design, construction, and characterization of a large synthetic human antibody phage display library. *Proteomics.* 2005;5(9):2340-2350.
 43. Schlothauer T, Herter S, Koller CF, et al. Novel human IgG1 and IgG4 Fc-engineered antibodies with completely abolished immune effector functions. *Protein Eng Des Sel.* 2016;29(10):457-466.
 44. Seckinger A, Delgado JA, Moser S, et al. Target expression, generation, preclinical activity, and pharmacokinetics of the BCMA-T cell bispecific antibody EM801 for multiple myeloma treatment. *Cancer Cell.* 2017;31(3):396-410.
 45. Bacac M, Colombetti S, Herter S, et al. CD20-TCB with obinutuzumab pretreatment as next-generation treatment of hematologic malignancies. *Clin Cancer Res.* 2018;24(19):4785-4797.
 46. Van Dijk JP, Knops GHJN, Van De Loch LTF, et al. Abnormal WT1 expression in the CD34-

- negative compartment in myelodysplastic bone marrow. *Br J Haematol*. 2002;118(4):1027-1033.
47. Krupka C, Kufer P, Kischel R, et al. CD33 target validation and sustained depletion of AML blasts in long-term cultures by the bispecific T-cell-engaging antibody AMG 330. *Blood*. 2014;123(3):356-365.
 48. Vick B, Rothenberg M, Sandhöfer N, et al. An advanced preclinical mouse model for acute myeloid leukemia using patients' cells of various genetic subgroups and in vivo bioluminescence imaging. *PLoS One*. 2015;10(3):e0120925.
 49. Lange T, Hubmann M, Burkhardt R, et al. Monitoring of WT1 expression in PB and CD34(+) donor chimerism of BM predicts early relapse in AML and MDS patients after hematopoietic cell transplantation with reduced-intensity conditioning. *Leukemia*. 2011;25(3):498-505.
 50. Holland CJ, Crean RM, Pentier JM, et al. Specificity of bispecific T cell receptors and antibodies targeting peptide-HLA. *J Clin Invest*. 2020;130(5):2673-2688.
 51. Tunger A, Wehner R, von Bonin M, et al. Generation of high-avidity, WT1-reactive CD8+ cytotoxic T cell clones with anti-leukemic activity by streptamer technology. *Leuk Lymphoma*. 2017;58(5):1246-1249.
 52. Greiner J, Ringhoffer M, Taniguchi M, et al. mRNA expression of leukemia-associated antigens in patients with acute myeloid leukemia for the development of specific immunotherapies. *Int J Cancer*. 2004;108(5):704-711.
 53. Anguille S, Van Tendeloo VF, Berneman ZN. Leukemia-associated antigens and their relevance to the immunotherapy of acute myeloid leukemia. *Leukemia*. 2012;26(10):2186-2196.
 54. Ley TJ, Miller C, Ding L, et al; Cancer Genome Atlas Research Network. Genomic and epigenomic landscapes of adult de novo acute myeloid leukemia. *N Engl J Med*. 2013;368(22):2059-2074.
 55. Cilloni D, Renneville A, Hermitte F, et al. Real-time quantitative polymerase chain reaction detection of minimal residual disease by standardized WT1 assay to enhance risk stratification in acute myeloid leukemia: a European LeukemiaNet study. *J Clin Oncol*. 2009;27(31):5195-5201.
 56. Rampal R, Figueroa ME. Wilms tumor 1 mutations in the pathogenesis of acute myeloid leukemia. *Haematologica*. 2016;101(6):672-679.
 57. Yamagami T, Sugiyama H, Inoue K, et al. Growth inhibition of human leukemic cells by WT1 (Wilms tumor gene) antisense oligodeoxynucleotides: implications for the involvement of WT1 in leukemogenesis. *Blood*. 1996;87(7):2878-2884.
 58. Ito K, Oji Y, Tatsumi N, et al. Antiapoptotic function of 17AA(+)WT1 (Wilms' tumor gene) isoforms on the intrinsic apoptosis pathway. *Oncogene*. 2006;25(30):4217-4229.
 59. Veomett N, Dao T, Liu H, et al. Therapeutic efficacy of an Fc-enhanced TCR-like antibody to the intracellular WT1 oncoprotein. *Clin Cancer Res*. 2014;20(15):4036-4046.
 60. Dubrovsky L, Pankov D, Brea EJ, et al. A TCR-mimic antibody to WT1 bypasses tyrosine kinase inhibitor resistance in human BCR-ABL+ leukemias. *Blood*. 2014;123(21):3296-3304.
 61. Dubrovina E, Carpenter T, Pankov D, Selvakumar A, Hasan A, O'Reilly RJ. Mapping of novel peptides of WT-1 and presenting HLA alleles that induce epitope-specific HLA-restricted T cells with cytotoxic activity against WT-1(+) leukemias. *Blood*. 2012;120(8):1633-1646.
 62. Berlin C, Kowalewski DJ, Schuster H, et al. Mapping the HLA ligandome landscape of acute myeloid leukemia: a targeted approach toward peptide-based immunotherapy [published correction appears in *Leukemia*. 2016;30(4):1003-1004]. *Leukemia*. 2015;29(3):647-659.
 63. Le Dieu R, Taussig DC, Ramsay AG, et al. Peripheral blood T cells in acute myeloid leukemia (AML) patients at diagnosis have abnormal phenotype and genotype and form defective immune synapses with AML blasts. *Blood*. 2009;114(18):3909-3916.
 64. Knaus HA, Berglund S, Hackl H, et al. Signatures of CD8+ T cell dysfunction in AML patients and their reversibility with response to chemotherapy. *JCI Insight*. 2018;3(21):e120974.
 65. Chiu H, Trisal P, Bjorklund C, et al. Combination lenalidomide-rituximab immunotherapy activates anti-tumour immunity and induces tumour cell death by complementary mechanisms of action in follicular lymphoma. *Br J Haematol*. 2019;185(2):240-253.
 66. Davies F, Baz R. Lenalidomide mode of action: linking bench and clinical findings. *Blood Rev*. 2010;24(suppl 1):S13-S19.
 67. Wang M, Fayad L, Wagner-Bartak N, et al. Lenalidomide in combination with rituximab for patients with relapsed or refractory mantle-cell lymphoma: a phase 1/2 clinical trial. *Lancet Oncol*. 2012;13(7):716-723.
 68. Salles G, Duell J, González Barca E, et al. Tafasitamab plus lenalidomide in relapsed or refractory diffuse large B-cell lymphoma (L-MIND): a multicentre, prospective, single-arm, phase 2 study. *Lancet Oncol*. 2020;21(7):978-988.
 69. Poh C, Frankel P, Ruel C, et al. Blinatumomab/lenalidomide in relapsed/refractory non-Hodgkin's lymphoma: a phase I California Cancer Consortium Study of safety, efficacy and immune correlative analysis. *Blood*. 2019;134(suppl 1):760.